Enhanced Performance of Photocatalytic Treatment of Congo Red Wastewater by CNTs-Ag Modified TiO_2 Under Visible Light

Yuewei Yang
Qufu Normal University
Kai Liu
Qufu Normal University
Fengfei Sun
Qufu Normal University
Yanyan Liu
Qufu Normal University
Junfeng Chen (chenjunfeng2011@163.com)
Qufu Normal University https://orcid.org/0000-0002-1277-7891

Research Article

Keywords: CNTs-Ag-TiO2 ternary composite, Photocatalysis, Degradation efficiency, Congo red wastewater, Visible light

Posted Date: August 13th, 2021

DOI: https://doi.org/10.21203/rs.3.rs-644698/v1

Version of Record: A version of this preprint was published at Environmental Science and Pollution Research on October 9th, 2021. See the published version at https://doi.org/10.1007/s11356-021-16734-w.

Abstract

In order to improve the treatment efficiency of printing and dyeing wastewater, the carbon nanotubes - silver modified -titanium dioxide (CNTs-Ag-TiO_2, CAT) ternary composite was prepared by a mechanical mixing method. It was found that the morphology of the prepared CAT sample was uniformly coated with strips of CNTs, speckled Ag and lumpy TiO_2.The (002) crystal plane of CNTs, the (101) crystal plane of TiO_2 and the (111) crystal plane of Ag were observed, which possessed functional groups such as Ti-OH and Ti-O-C, indicating that the prepared CAT sample had photocatalytic reaction sites. The visible light utilization of titanium dioxide can be improved. The treatment effect of different proportions of CNTs-Ag-TiO_2 on Congo red wastewater was tested, and the results showed that the optimum degradation effect of Congo red wastewater was CNTs: Ag = 10:1, and the treated amount of CNTs/Ag was 15%, and the removal rate of Congo red wastewater could reach 100% within 140min. The excellent removal effect of CAT ternary composite on Congo red wastewater provided a new idea and way for the modification of TiO_2 and its composites for the potential of organic dyes degradation.

Introduction

Printing and dyeing wastewater was one of the main sources of industrial wastewater, which discharge a large number of colored wastewater with various components. Organic dyes, which produce printing and dyeing wastewater, had a wide range of uses in many industries, including textiles, leather, paper, printing, cosmetics and plastics(Wang et al. 2019). Most of these dyes had the characteristics of stable structure, difficult degradation and high toxicity, which had brought serious problems to the environment(Eltaweil et al. 2021). Congo red (CR) was a typical azo dye (benzidine direct azo anion), and its metabolite benzidine was a known carcinogen, which had caused serious harm to human health(Yang et al. 2017).

At present, the methods of removing organic dyes from wastewater mainly include physical adsorption(Hou et al. 2021), chemical oxidation(Xi et al. 2021), acoustic catalysis(Chai et al. 2020), photocatalytic degradation, etc.(Rizal et al. 2021). Physical adsorption, its principle was that adsorbent and pollutants would reach adsorption equilibrium, and the process was reversible, which could not completely remove pollutants and might cause secondary pollution. Chemical method had the advantages of rapid reaction and thorough degradation, but its cost was often higher, and other toxic by-products might be produced in the chemical reaction, causing harm to the environment. These shortcomings limit their application in the treatment of printing and dyeing wastewater. Therefore, we urgently need an environmentally friendly, economical and efficient purification method.

The appearance of photocatalytic technology had brought new hope to industrial wastewater treatment. This technology aimed to make photocatalyst produce active particles with redox ability by sunlight to oxidize and decompose pollutants, and the whole process was environmentally friendly and non-toxic(Mohammed et al. 2021). TiO_2 semiconductor material was the photocatalyst with the most natural affinity. Due to its high catalytic activity, low cost and stable chemical properties, it had received extensive attention in the field of environmental governance(Sheng et al. 2020). TiO_2 catalyst had strong oxidation

capacity, which could oxidize some toxic and not easily degradable pollutants, and eventually transform them into non-toxic and harmless small molecule. It could effectively protect the environment and personal safety, and was a very ideal photocatalyst(Arfanis et al. 2017; Athanasekou et al. 2017). Brooke et al found that compared with ultraviolet photolysis alone, TiO_2 photocatalysis under ultraviolet (UV) irradiation significantly improved the removal rate of aromatic macromolecular organic compounds(Mayer et al. 2019). Using UV- TiO_2 to treat the mixed wastewater of urban and textile dyes was very effective for removing color and other organic compounds. The metal-metal co-doping changed the band gap energy and the structure of co-doped nanoparticles, which showed higher photocatalytic activity. The silicon-tungsten co-doped titanium dioxide had a positive effect on the photocatalytic degradation of methyl orange dye under 40 W low-pressure mercury lamp(Xu et al. 2018; El Mragui et al. 2019).

The surface modification of TiO_2 could extend the light absorption capacity to visible wavelengths, increase the utilization of visible light, improve the separation of photogenerated electron hole pairs, enhance the overall efficiency of CO_2 photoconversion process and reduce the processing cost(Athanasekou et al. 2018). It was found that plasma metal Ag and Au loaded on TiO_2 could form resonance, caused intense oscillation of surface electrons, and transfer hot electrons generated on the metal surface to TiO_2 and induce photocatalytic reaction(Low et al. 2017). As the plasma absorption of Au and Ag lies in the visible light range, these visible light active plasma metals could be used as visible photosensitizers for TiO_2. At the same time, the Schottky potential barrier formed when the noble metal particles were in contact with the semiconductor could effectively inhibit the recombination of hole-electron pairs and increase the photocatalytic activity(Chen et al. 2020). Therefore, precious metal deposition could not only improve the separation of photo-generated carriers, but also boost the utilization rate of visible light due to local ionic resonance.

It was necessary to find a carrier for photocatalyst because nanoparticles were easy to agglomerate and hinder the photocatalytic performance. Carbon nanotubes, with large specific surface area and layered hollow structure, were a new adsorbent with unique mechanical, electrical and thermal properties. Several studies had shown that the photocatalytic degradation rate was closely related to the concentration of pollutants adsorbed on the catalyst surface, so carbon nanotubes (CNTs) could be used as carriers to adsorb pollutants and effectively separate photogenerated hole-electron pairs(Djellabi et al. 2019; Tibodee et al. 2019; Chávez et al. 2020). By combining TiO_2, precious metal and CNTs, not only improved the light absorption efficiency of TiO2, but also promoted the degradation of pollutants (Peng et al. 2016). However, there were currently few studies on the modification of TiO2 with precious metals and nano-carbon. Most of the research on modified TiO2 ternary composite materials focused on semiconductor materials and nanomaterials with good conductivity. Fu et al. synthesized a three-dimensional (3D) photocatalyst by self-assembly of graphite carbon nitride (g-C3N4), titanium dioxide (TiO_2), graphene (Gr) and carbon nanotubes (CNTs). Highly interconnected carbon nanotubes could not only effectively promote the transfer of photo-generated charge carriers, but also provide a larger specific surface area for photoreaction, which had a remarkable effect in phenol degradation experiments(Fu et

al. 2020). Huang et al. synthesized a novel carbon nanotube/titanium dioxide/zinc oxide composite material, which showed significant degradation effect of rhodamine B under visible light(Huang et al. 2018).

In this study, CNTs-Ag-TiO_2 ternary composite was prepared by a mechanical mixing method, and the treatment effects of CNTs-Ag-TiO_2 with different proportions on CR were studied, and the best ratio of the ternary composites was found out. The structure of the composites was characterized by X-ray diffraction (XRD) and Fourier transform infrared spectroscopy (FTIR), and the morphology of the composites was analyzed by field emission scanning electron microscopy (SEM) and energy dispersive spectroscopy (EDS). The degradation mechanism was analyzed by X-ray diffraction (XRD) and Fourier transform infrared spectroscopy (FTIR) spectra before and after the reaction. This paper not only studied the degradation efficiency of CR by this composite material, but also provided experimental basis and theoretical support for the modification of TiO_2 and its composites for the potential of organic dyes degradation.

Materials And Methods

2.1 Preparation of CNTs-Ag-TiO_2 (CAT) nano-composite

2.1.1 Pretreatment of carbon nanotubes (CNTs)

The modified CNTs were prepared by measuring 0.5g CNTs (MWCNTs, purity > 95%, Beijing, China) into the mixed solution of 10mL concentrated nitric acid (HNO_3, purity > 65%, Yantai, China) and 30mL concentrated sulfuric acid (H_2SO_4, purity > 95%, Yantai, China), and the suspension was stirred at 300 r/min for 30min and heated to 80℃, The oxidized CNTs were washed the mixture solution with deionized water to neutrality, taken out the solid and drying at 70°C, and stored in containers for subsequent use.

2.1.2 Preparation of carbon nanotube-silver (CNTs-Ag, CA) binary composites

The modified CNTs and nano silver powder (AgNPs, purity > 99%, Shanghai, China) were added into 30mL absolute ethyl alcohol (purity > 95%, Shandong, China) at the same time according to a certain proportion, and the CNTs-Ag composite material was obtained by standing after ultrasonic treatment for 30min, taking out the solid after centrifugal treatment for 5min, and grinding. To explore the influence of different Ag loading on CNTs on the treatment effect of ternary material CNTs-Ag-TiO_2, CA materials with CNTs-Ag ratio of 20:1, 10:1 and 5:1 were prepared respectively, and their degradation performance on CR was tested under the same conditions.

2.1.3 Synthesis of CNTs-Ag-TiO_2 (CAT) ternary composites

0.1g TiO_2 (TiO_2, purity > 98%, Sinopharm, China) powder was put into 30mL absolute ethyl alcohol for ultrasound 30min marked as solution A, a certain amount of prepared CA material was added into 1.2mL of sodium dodecyl benzene sulfonate aqueous solution with mass fraction of 2%, then 20mL absolute ethyl alcohol was added into it, and ultrasound 30min marked as solution B. The A solution is slowly added to the B solution, magnetic stirring and ultrasonic for 30minand the suspension was centrifuged for 5min, followed by drying in an oven at 70°C for 48 h. In order to explore the best compounding ratio, CAT samples with CA content of 5%, 10%, 15% and 20% were prepared. At the same time, CNTs- TiO_2 (CT) samples with the same mass percentage were prepared for comparative study. The flow chart of material preparation is shown in Fig. 1.

2.2 Characterization

The FESEM (Hitachi S-4800) and EDS (Oxford 6498) were used to characterize the micromorphology and element distribution of the samples. A XRD (MiniFlex600) was used to test the crystal structure of the prepared materials, and FTIR (NEXUS-470) was used to detect the surface functional groups of the materials in the wave number range of 4000 – 400 cm^{-1}.

2.3 Photocatalytic degradation experiment

In this experiment, CR wastewater was used to simulate printing and dyeing wastewater. 100mL CR solution with a concentration of 100mg/L was taken and 50mg CAT sample was added to it. The sample stirred in the dark for further 60 min in order to attain the adsorption-desorption equilibrium and to ensure that the removal of dye was completed by the photocatalytic process. The degradation performance of CAT on CR wastewater under 1000W xenon lamp was tested in photochemical reaction device (HF-GHX-II). The concentration of CR wastewater solution was measured every 10 minutes with a dual-beam (UV-8000s) spectrophotometer. The adsorption-photocatalytic degradation effect was determined by the ratio of the CR wastewater concentration C_t to the initial concentration C_0 at the corresponding time. That is, the degradation efficiency is denoted by C_t/C_0.

Results And Discussion

3.1 Morphology and structure of CAT

Fig. 2 showed the SEM images of the synthesized CAT composites with different proportions. When the mass ratio was 20:1, the SEM image of CA sample was shown in Fig 2a, and the amount of AgNPs coated on CNTs surface was less, that was, most CNTs surface has no AgNPs. This was mainly because the content of treated nano silver was too low to effectively adhere to the surface of CNTs. When the mass ratio increased to 10:1, as shown in Fig. 2b, the number of silver particles on the surface of CNTs increased significantly. However, when the proportion of CNTs/Ag was increased to 5:1, as shown in Fig. 2c, the coating effect on CNTs does not further improve. This was mainly because too much nano-silver was easy to cause agglomeration, resulting in poor loading effect. Comparing the morphologies, it was considered that the CNTs /Ag was 10:1, the CA composite with uniform surface coating of AgNPs could

be obtained. When the content of CA was 10%, only a small amount of CA material could be seen from Figure 2d, which indicates that TiO_2 was not uniformly dispersed on the surface of CA, which might be due to the low content of CA, which could not provide sufficient active sites, which makes TiO_2 particles agglomerate together. When the content of CA was 15% and 20%, as shown in Fig. 2e and 2f, the outline of carbon tubes was clearer, and TiO_2 loaded on the surface was not agglomerated on a large scale, indicating that TiO_2 particles were well attached to the surface of samples. In order to further determine the dispersion uniformity of the composite material, the energy spectrum analysis of CAT samples with 10% CA content was tested. The EDX spectrum of nanocomposite was depicted in Fig. 3, confirming the presence of Ti and AgNPs. The sample showed that TiO_2 was evenly dispersed, and AgNPs coated on CNTs surface well, the three components were evenly distributed.

The peak position and strength of the sample FTIR could be used to reflect the changes of functional groups on the surface of the prepared nanocomposites. As shown in Fig. 4a, CNTs showed a characteristic strong vibration band at 3430cm^{-1}, which was attributed to the stretching of -COOH group and OH adsorbed water molecules. The bands at 1420cm^{-1} were attributed to the OH deformation vibration of -COOH group. The bands at 1640cm^{-1}were attributed to the C=O tensile vibrations. The bands at 1212-1175cm^{-1} and 1112-1038cm^{-1} were attributed to -C-O tensile vibrations. These peaks confirmed the introduction of the -COOH group in the acid treatment of CNTs(Natarajan et al. 2017). In CAT materials, the strength of vibration bands at 3430 and 1623cm^{-1} weakened as they move towards the low wave number at 3424 and 1567cm^{-1}, indicating that the deformation vibration of O-H was replaced by the deformation vibration of Ti-OH on the surface of CNTs. The wide absorption bands between 1000 and 500cm^{-1} were attributed to the bending vibrations of the Ti-O-Ti and Ti-O-C bonds. The shift of the C-O bond's absorption band from 1093 to 1115cm^{-1} was also attributed to the tensile vibration of the Ti-O-C bond(Azzam et al. 2019).

The crystal structure of the composite samples was characterized by XRD. Used to determine whether the mixing process has an effect on the crystal structure of the sample. As shown in Fig. 4b, there were obvious diffraction peaks at 2θ of 38.1°, 44.2°, 64.40° and 77.4°, corresponding to the (111), (200), (220) and (311) crystal faces of Ag (JCPDS No.04-0783).There were obvious diffraction peaks at 2θ of 25.3°, 38.6°, 48.1°, 53.90°, 55.1° and 62.7°, corresponding to the (101), (004), (200), (105), (211) and (204) crystal faces of anatase phase TiO_2 (JCPDS No. 21-1272), respectively. In the XRD pattern of CA samples, when 2θ was 25.8°, the characteristic diffraction peak of CNTs was observed, which corresponds to the (002) crystal plane of typical graphite sheet(Zhou et al. 2020). However, there was no diffraction peak corresponding to CNTs in the XRD pattern of CAT samples, which might be the proximity between the main characteristic peak of CNTs at 25.8° and the main peak of anatase TiO_2 at 25.3°, resulting in the overlapping of diffraction peaks and the increase of peak width(Ahmad et al. 2017; Zhou et al. 2020). The diffraction peak of Ag was obvious in the XRD pattern of CAT samples, and we could see the diffraction peaks of Ag and TiO_2 were very close (Ag (111) and TiO_2 (004)) (Chaudhary et al.

2017; Tan et al. 2017; Zhang et al. 2019). The results clearly indicated that the prepared CAT sample had photocatalytic reaction sites.

3.2 Degradation performance of CAT on CR wastewater

In order to explore the photocatalytic performance of CAT sample under visible light, the treatment effect of CNTs/Ag with different proportions of CAT and the ability of CAT with different CA content to degrade CR wastewater were tested under visible light, and the results were shown in Figure 5. The uniformity of CA composites was affected by different CNTs/Ag ratios. As shown in Fig. 5a, CR wastewater was completely degraded within 150 minutes when CNTs/Ag ratio was 10:1. This was because the CA composite with AgNPs coated on the surface was uniform. Therefore, in the prepared CAT sample with CA treated content of 15%, AgNPs were better dispersed on the surface of the sample, so that the role of Ag as an induced electron could be better exerted, the electron-space separation efficiency of TiO_2 could be improved, and the degradation effect of TiO_2 on CR wastewater could be promoted(Espino-Estévez et al. 2016). Different treated amounts of CA had a direct impact on CAT degradation of CR wastewater, as shown in Fig. 5b. Due to the separation of photogenerated electrons by Ag as visible photosensitizer and CNTs, CAT sample degradation rate of CR wastewater could reach 90% when CA treated amount was 10%. With the increase of CA treated amount, the treatment effect first increased and then decreased. The maximum removal effect was obtained when the content of CA was 15%, and 100mL of CR wastewater with a concentration of 100mg/L could be degraded in 140min. When the mass fraction of CA was 20%, the treatment effect was not as good as 15% CA. The possible reason was that the excessive CA content reduces the uniformity of the TiO_2 coating, affects the absorption of photons by TiO_2, produces a shielding effect, and affects the degradation efficiency. The removal rate of CR wastewater in CT samples with mass fraction of 15% prepared by CNTs and TiO_2 was 82%. The reason was that TiO_2 nanoparticles were attached to the sidewall of CNTs, which made TiO_2 and CNTs in a good bonding state at the interface, and the formed Ti-O-C bond separates the photogenerated hole-electron pair and reduces the band gap width. Therefore, the catalytic activity of CT samples was improved, the absorption of visible light was significantly enhanced, and the photocatalytic performance of composite materials was improved(Zhao et al. 2020). In addition, on the one hand CNTs could be used as a carrier of photocatalytic reaction to block photo-generated hole-electron recombination, and on the other hand, Ti-O-C could be formed to expand the interface area and improve the degradation effect of CR wastewater in CT samples under visible light, when 15%CT samples degrade CR wastewater (Nguyen et al. 2016).

3.3 Number of reuses for CAT degradation on CR wastewater

To study the stability of CAT samples with CNTs/Ag ratio of 10:1 and CA treated ratio of 15%, repeated cyclic degradation experiments were carried out, and the results were shown in Fig.6. After the catalytic degradation was finished, the catalyst was repeatedly washed with deionized water, and the catalytic degradation experiment was carried out again in the same environment, repeated five times. It could be found that the degradation efficiency of 15% CAT remained stable in the first four experiments, and

decreased slightly in the fifth experiment, which indicated that 15% CAT had high catalytic performance and excellent stability.

3.4 Photocatalytic degradation mechanism of CAT

In order to further determine the degradation mechanism of CAT composites, FTIR and XRD of CAT samples with 15% CA treated after reaction were measured. As shown in Fig. 7a, CAT showed a characteristic strong vibration band at 3424 and 1567cm^{-1}, and the tensile strength of Ti-OH group and OH adsorbed by water molecules decreases, which might be the reaction between activated electron holes and adsorbed water or OH^- to form highly active superoxide radical ions, thus achieving the effect of catalytic degradation(Jung et al. 2015). After the end of the reaction, the absorption bands of CAT at 3424 and 1567cm^{-1} might be related to the formation of OH formed by hydrogen bonds between the benzene ring on the surface of CNTs and organics containing oxygen functional groups(Zhao et al. 2018). The bending vibration strength of the Ti-O-Ti and Ti-O-C bonds in the wide absorption band between 1000 and 500cm^{-1} was weakened, and the tensile vibration strength of the -C-O bond in the absorption band between 1112-1038cm^{-1} was weakened. This was attributed to the adsorption of CR wastewater onto CNTs by complexation with oxygen-containing functional groups. Therefore, the adsorption mechanism of CNTs for CR wastewater might include the electrostatic adsorption on the sample surface, π-π interaction and the complexation of oxygen-containing functional groups of the adsorbents(Wang et al. 2015). The bending vibration intensity of T-O-C bond was weakened, which indicated that Ag was mainly used as photosensitizer in the photocatalysis of samples, which played an important role in the efficient photocatalytic activity of TiO_2 under visible light. It was found from Fig. 7b that the structure of CAT composite had not changed obviously during the photocatalytic reaction, which indicated that TiO_2, Ag and CNTs were only carriers of photo-generated electron transfer in the photocatalytic reaction, and their own structure had not changed. The oxidation-reduction reaction with organic pollutants was mainly caused by superoxide radicals with high activity(El Mragui et al. 2021). CNTs mainly played a role in the separation of photogenerated electrons. Due to the local surface plasmonic resonance effect of Ag , it could not only improve the separation of photogenerated charge carriers, but also generate hot electrons transfer to TiO_2 and induce photocatalytic reaction, which improved the utilization rate of TiO_2 for visible light(Chen et al. 2021). Therefore, the photocatalytic reaction of the prepared CAT ternary composites under visible light may be as follows: visible light resonates with Ag, and electrons are injected into the TiO_2 conduction band. At the same time, the Ti-O-C bond formed by TiO_2 and CNTs reduces the band gap width, so that the electrons in the TiO_2 conduction band were excited, and the excited electrons were further transferred by a well-conducted Ag and CNTs to promotes the separation of electron holes. When electrons and holes flow, a Schottky potential barrier was formed at the interface between Ag and TiO_2, which inhibits the recombination of electron holes in the degradation process and further improves the catalytic activity of CAT materials in visible light.

Conclusions

In this paper, CNTs-Ag- TiO_2 ternary composites were prepared by a mechanical mixing method. By using the good adsorption ability, electron transfer ability and visible light photosensitization activity of CA material, the degradation ability of the composites to organic pollutants under visible light was improved. The best treated ratio of this ternary material was explored. The CA material with good morphology and uniform package was prepared by mixing CNTs and Ag at a ratio of 10:1, and the CAT ternary composite nano material prepared by adding 15% CA sample to TiO_2 could degrade CR wastewater completely in 140min under visible light. By characterizing the structure of the samples before and after the reaction, the possible mechanism of photocatalytic treatment of CR wastewater by CNTs-Ag modified TiO_2 under visible light was expounded. The adsorption mechanism of CNTs on CR wastewater includes electrostatic adsorption, π-π interaction and complexation. The role of CNTs in photocatalysis mainly includes providing highly active superoxide radicals and separating photogenerated electrons. Ag could not only improve the separation of photo-generated charge carriers, but also increase the utilization rate of visible light of TiO_2 as a visible photosensitizer. In addition, the prepared CAT ternary composite material had stable structure in photocatalysis experiment, did not produce intermediate products, and could be reused. The action mechanism of CAT ternary composite material was determined in the photocatalytic degradation of organic matter, which would provide a new idea and way for the modification of TiO_2 and its composites for the potential of organic dyes degradation.

Declarations

Author contribution: Y. Y., K. L. and J.C. conceived and designed the experiments. The experiments were performed by Y. Y., K. L. F. S., Y. L. and J. C. Data was analyzed by Y. Y., K. L. F. S., Y. L. and J. C. The paper was written by Y. Y., K. L. and J.C.

Funding: This work was supported by Shandong Provincial Natural Science Foundation (ZR2020QC048 and ZR2019BB040), Postdoctoral Science Foundation of China (2021M691850), the National Natural Science Foundation of China (NO. 31901188 and NO. 31672314).

Data availability: We declare that the data supporting the findings of this study are available within the article.

Materials availability: We declare that the materials supporting the findings of this study are available within the article.

Declarations

Ethics approval and consent to participate: No applicable

Consent for publication: Not applicable.

Competing interests: The authors declare no competing interests.

References

1. Ahmad A, Razali MH, Mamat M, et al (2017) Adsorption of methyl orange by synthesized and functionalized-CNTs with 3-aminopropyltriethoxysilane loaded TiO2 nanocomposites. Chemosphere 168:474–482. https://doi.org/10.1016/j.chemosphere.2016.11.028
2. Arfanis MK, Adamou P, Moustakas NG, et al (2017) Photocatalytic degradation of salicylic acid and caffeine emerging contaminants using titania nanotubes. Chem Eng J 310:525–536. https://doi.org/10.1016/j.cej.2016.06.098
3. Athanasekou C, Romanos GE, Papageorgiou SK, et al (2017) Photocatalytic degradation of hexavalent chromium emerging contaminant via advanced titanium dioxide nanostructures. Chem Eng J 318:171–180. https://doi.org/10.1016/j.cej.2016.06.033
4. Athanasekou CP, Likodimos V, Falaras P (2018) Recent developments of TiO2 photocatalysis involving advanced oxidation and reduction reactions in water. J Environ Chem Eng 6:7386–7394. https://doi.org/10.1016/j.jece.2018.07.026
5. Azzam EMS, Fathy NA, El-Khouly SM, Sami RM (2019) Enhancement the photocatalytic degradation of methylene blue dye using fabricated CNTs/TiO 2 /AgNPs/Surfactant nanocomposites. J Water Process Eng 28:311–321. https://doi.org/10.1016/j.jwpe.2019.02.016
6. Chai YD, Pang YL, Lim S, Chong WC (2020) Sonocatalytic degradation of Congo Red using biomass-based cellulose/TiO2 composite. Mater Today Proc. https://doi.org/10.1016/j.matpr.2020.09.246
7. Chaudhary D, Singh S, Vankar VD, Khare N (2017) A ternary Ag/TiO2/CNT photoanode for efficient photoelectrochemical water splitting under visible light irradiation. Int J Hydrogen Energy 42:7826–7835. https://doi.org/10.1016/j.ijhydene.2016.12.036
8. Chávez AM, Solís RR, Beltrán FJ (2020) Magnetic graphene TiO2-based photocatalyst for the removal of pollutants of emerging concern in water by simulated sunlight aided photocatalytic ozonation. Appl Catal B Environ 262:118275. https://doi.org/10.1016/j.apcatb.2019.118275
9. Chen M, Wang H, Chen X, et al (2020) High-performance of Cu-TiO2 for photocatalytic oxidation of formaldehyde under visible light and the mechanism study. Chem Eng J 390:124481. https://doi.org/10.1016/j.cej.2020.124481
10. Chen Q, Wang K, Gao G, et al (2021) Singlet oxygen generation boosted by Ag–Pt nanoalloy combined with disordered surface layer over TiO2 nanosheet for improving the photocatalytic activity. Appl Surf Sci 538:147944. https://doi.org/10.1016/j.apsusc.2020.147944
11. Djellabi R, Yang B, Wang Y, et al (2019) Carbonaceous biomass-titania composites with Ti–O–C bonding bridge for efficient photocatalytic reduction of Cr(VI) under narrow visible light. Chem Eng J 366:172–180. https://doi.org/10.1016/j.cej.2019.02.035
12. El Mragui A, Zegaoui O, Daou I (2019) Synthesis, characterization and photocatalytic properties under visible light of doped and co-doped TiO2-based nanoparticles. Mater Today Proc 13:857–865. https://doi.org/10.1016/j.matpr.2019.04.049

13. El Mragui A, Zegaoui O, Esteves da Silva JCG (2021) Elucidation of the photocatalytic degradation mechanism of an azo dye under visible light in the presence of cobalt doped TiO2 nanomaterials. Chemosphere 266:128931. https://doi.org/10.1016/j.chemosphere.2020.128931
14. Eltaweil AS, Elshishini HM, Ghatass ZF, Elsubruiti GM (2021) Ultra-high adsorption capacity and selective removal of Congo red over aminated graphene oxide modified Mn-doped UiO-66 MOF. Powder Technol 379:407–416. https://doi.org/10.1016/j.powtec.2020.10.084
15. Espino-Estévez MR, Fernández-Rodríguez C, González-Díaz OM, et al (2016) Effect of TiO2-Pd and TiO2-Ag on the photocatalytic oxidation of diclofenac, isoproturon and phenol. Chem Eng J 298:82–95. https://doi.org/10.1016/j.cej.2016.04.016
16. Fu Z, Wang H, Wang Y, et al (2020) Construction of three-dimensional g-C3N4/Gr-CNTs/TiO2 Z-scheme catalyst with enhanced photocatalytic activity. Appl Surf Sci 510:. https://doi.org/10.1016/j.apsusc.2020.145494
17. Hou F, Wang D, Ma X, et al (2021) Enhanced adsorption of Congo red using chitin suspension after sonoenzymolysis. Ultrason Sonochem 70:105327. https://doi.org/10.1016/j.ultsonch.2020.105327
18. Huang Y, Li R, Chen D, et al (2018) Synthesis and characterization of CNT/TiO2/ZnO composites with high photocatalytic performance. Catalysts 8:1–6. https://doi.org/10.3390/catal8040151
19. Jung JY, Lee D, Lee YS (2015) CNT-embedded hollow TiO2 nanofibers with high adsorption and photocatalytic activity under UV irradiation. J Alloys Compd 622:651–656. https://doi.org/10.1016/j.jallcom.2014.09.068
20. Low J, Cheng B, Yu J (2017) Surface modification and enhanced photocatalytic CO 2 reduction performance of TiO 2 : a review. Appl Surf Sci 392:658–686. https://doi.org/10.1016/j.apsusc.2016.09.093
21. Mayer BK, Johnson C, Yang Y, et al (2019) From micro to macro-contaminants: The impact of low-energy titanium dioxide photocatalysis followed by filtration on the mitigation of drinking water organics. Chemosphere 217:111–121. https://doi.org/10.1016/j.chemosphere.2018.10.213
22. Mohammed AM, Mohtar SS, Aziz F, et al (2021) Ultrafast degradation of Congo Red dye using a facile one-pot solvothermal synthesis of cuprous oxide/titanium dioxide and cuprous oxide/zinc oxide p-n heterojunction photocatalyst. Mater Sci Semicond Process 122:105481. https://doi.org/10.1016/j.mssp.2020.105481
23. Natarajan TS, Lee JY, Bajaj HC, et al (2017) Synthesis of multiwall carbon nanotubes/TiO2 nanotube composites with enhanced photocatalytic decomposition efficiency. Catal Today 282:13–23. https://doi.org/10.1016/j.cattod.2016.03.018
24. Nguyen KC, Ngoc MP, Nguyen M Van (2016) Enhanced photocatalytic activity of nanohybrids TiO2/CNTs materials. Mater Lett 165:247–251. https://doi.org/10.1016/j.matlet.2015.12.004
25. Peng K, Fu L, Yang H, Ouyang J (2016) Perovskite LaFeO3/montmorillonite nanocomposites: Synthesis, interface characteristics and enhanced photocatalytic activity. Sci Rep 6:1–10. https://doi.org/10.1038/srep19723

26. Rizal MY, Saleh R, Prakoso SP, et al (2021) Ultraviolet- and visible-light photocatalytic and sonophotocatalytic activities toward Congo red degradation using Ag/Mn3O4 nanocomposites. Mater Sci Semicond Process 121:105371. https://doi.org/10.1016/j.mssp.2020.105371
27. Sheng W, Shi JL, Hao H, et al (2020) Selective aerobic oxidation of sulfides by cooperative polyimide-titanium dioxide photocatalysis and triethylamine catalysis. J Colloid Interface Sci 565:614–622. https://doi.org/10.1016/j.jcis.2020.01.046
28. Tan P, Chen X, Wu L, et al (2017) Hierarchical flower-like SnSe2 supported Ag3PO4 nanoparticles: Towards visible light driven photocatalyst with enhanced performance. Appl Catal B Environ 202:326–334. https://doi.org/10.1016/j.apcatb.2016.09.033
29. Tibodee A, Pannak P, Akkarachaneeyakorn K, et al (2019) Use of the graphite intercalation compound to produce low-defect graphene sheets for the photocatalytic enhancement of graphene/TiO2 composites. Mater Chem Phys 235:121755. https://doi.org/10.1016/j.matchemphys.2019.121755
30. Wang Y, Dai X, Zhan Y, et al (2019) In situ growth of ZIF-8 nanoparticles on chitosan to form the hybrid nanocomposites for high-efficiency removal of Congo Red. Int J Biol Macromol 137:77–86. https://doi.org/10.1016/j.ijbiomac.2019.06.195
31. Wang Y, Zhu J, Huang H, Cho HH (2015) Carbon nanotube composite membranes for microfiltration of pharmaceuticals and personal care products: Capabilities and potential mechanisms. J Memb Sci 479:165–174. https://doi.org/10.1016/j.memsci.2015.01.034
32. Xi J, Wang Q, Duan X, et al (2021) Continuous flow reduction of organic dyes over Pd-Fe alloy based fibrous catalyst in a fixed-bed system. Chem Eng Sci 231:116303. https://doi.org/10.1016/j.ces.2020.116303
33. Xu M, Mao Y, Song W, et al (2018) Preparation and characterization of Fe-Ce co-doped Ti/TiO2 NTs/PbO2 nanocomposite electrodes for efficient electrocatalytic degradation of organic pollutants. J Electroanal Chem 823:193–202. https://doi.org/10.1016/j.jelechem.2018.06.007
34. Yang M, Wu Y, Rao R, Wang H (2017) Methanol promoted synthesis of porous hierarchical α-Ni(OH)2 for the removal of Congo red. Powder Technol 320:377–385. https://doi.org/10.1016/j.powtec.2017.07.074
35. Zhang Y, Yuan C, Wang Q, et al (2019) Photoelectrochemical activity of CdS/Ag/TiO2 nanorod composites: Degradation of nitrobenzene coupled with the concomitant production of molecular hydrogen. Electrochim Acta 328:135124. https://doi.org/10.1016/j.electacta.2019.135124
36. Zhao C, Guo J, Yu C, et al (2020) Fabrication of CNTs-Ag-TiO2 ternary structure for enhancing visible light photocatalytic degradation of organic dye pollutant. Mater Chem Phys 248:122873. https://doi.org/10.1016/j.matchemphys.2020.122873
37. Zhao L, Deng J, Sun P, et al (2018) Nanomaterials for treating emerging contaminants in water by adsorption and photocatalysis: Systematic review and bibliometric analysis. Sci Total Environ 627:1253–1263. https://doi.org/10.1016/j.scitotenv.2018.02.006
38. Zhou N, Wu Y, Li Y, et al (2020) Interconnected structure Si@TiO2-B/CNTs composite anode applied for high-energy lithium-ion batteries. Appl Surf Sci 500:144026.

https://doi.org/10.1016/j.apsusc.2019.144026

Figures

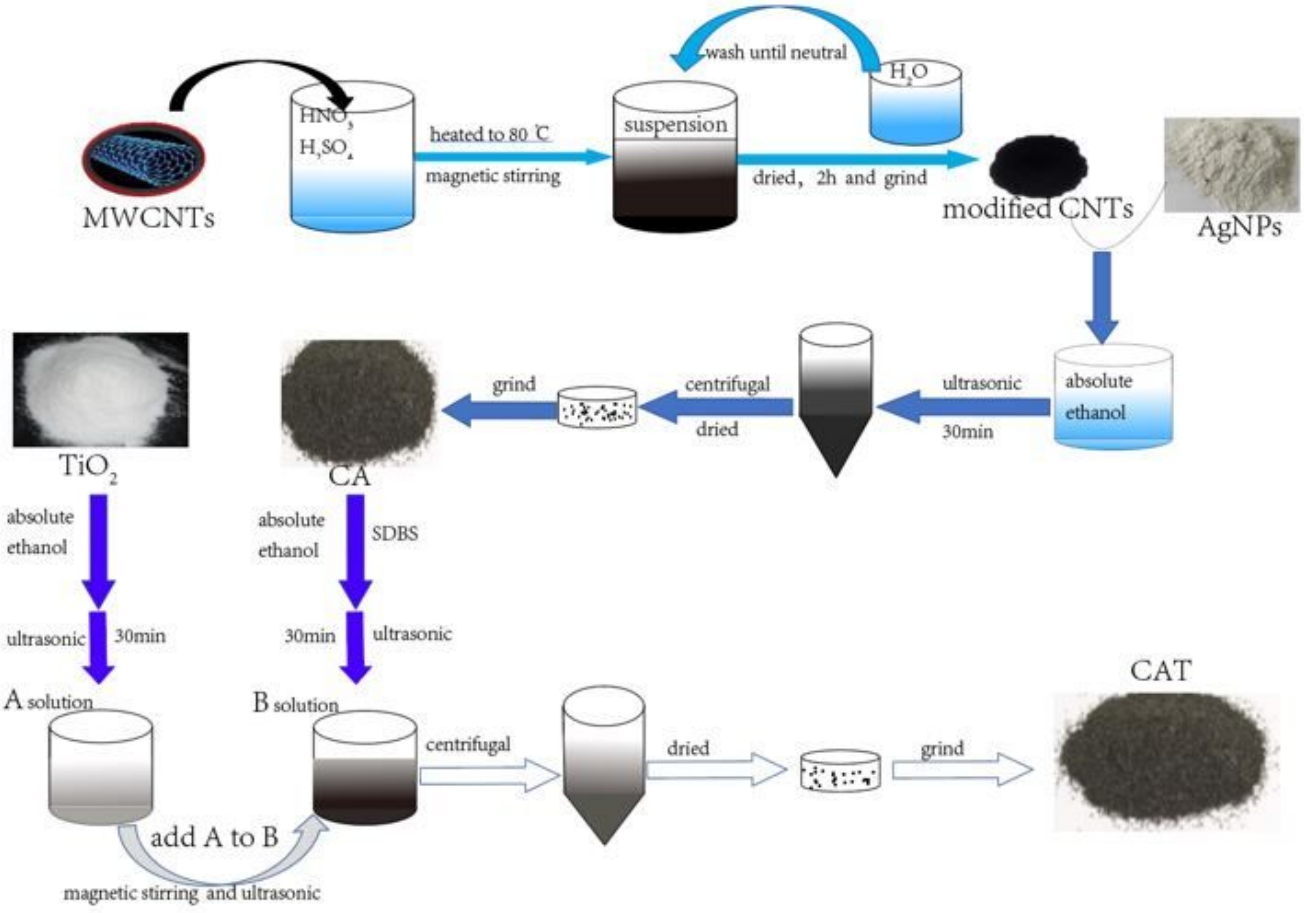

Figure 1

Schematic for the preparation of CAT samples.

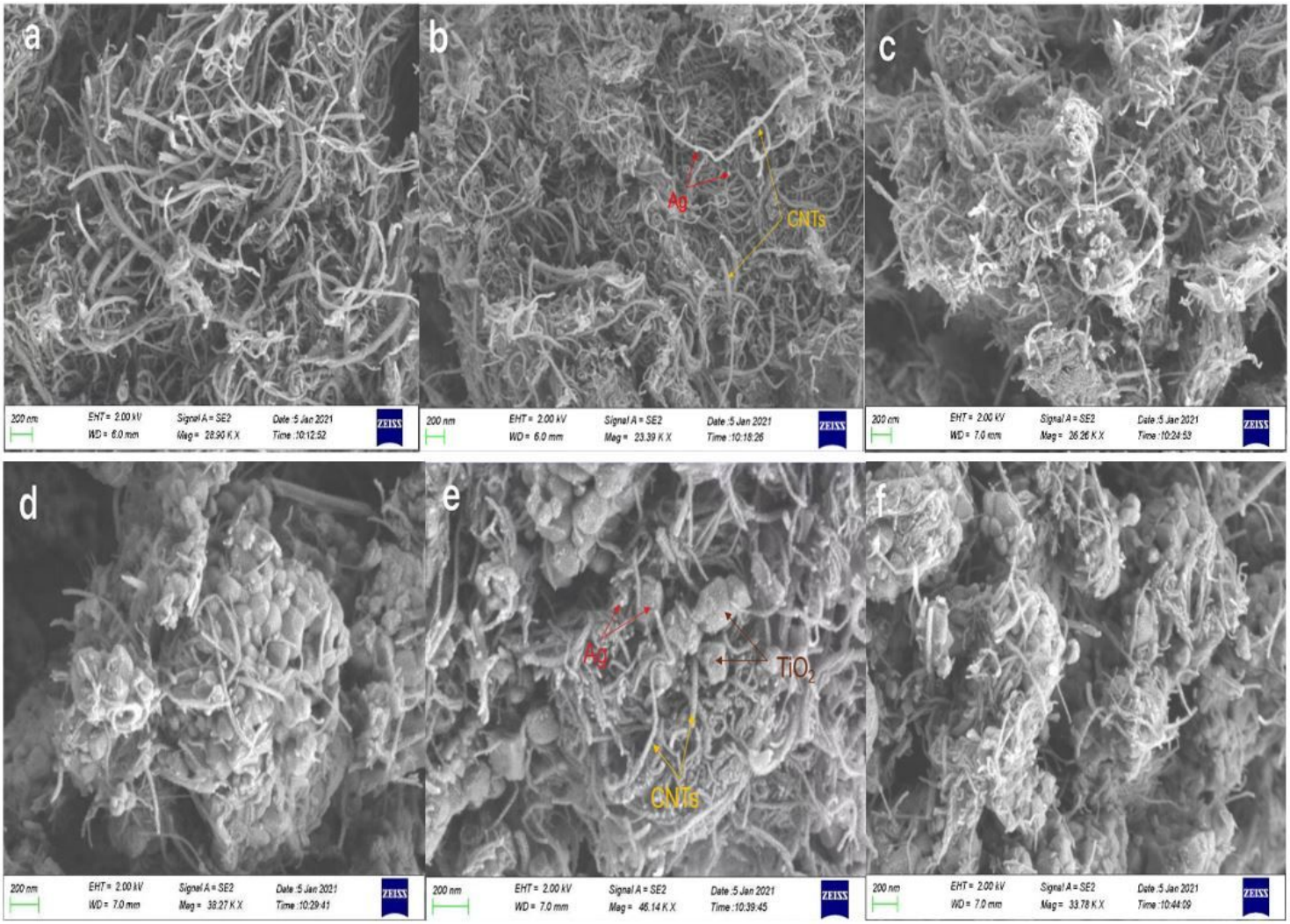

Figure 2

SEM images of CAT products with different treated ratios (a)20:1 (b)10:1 (c)5:1 CA and d 10% e 15% (f)20%.

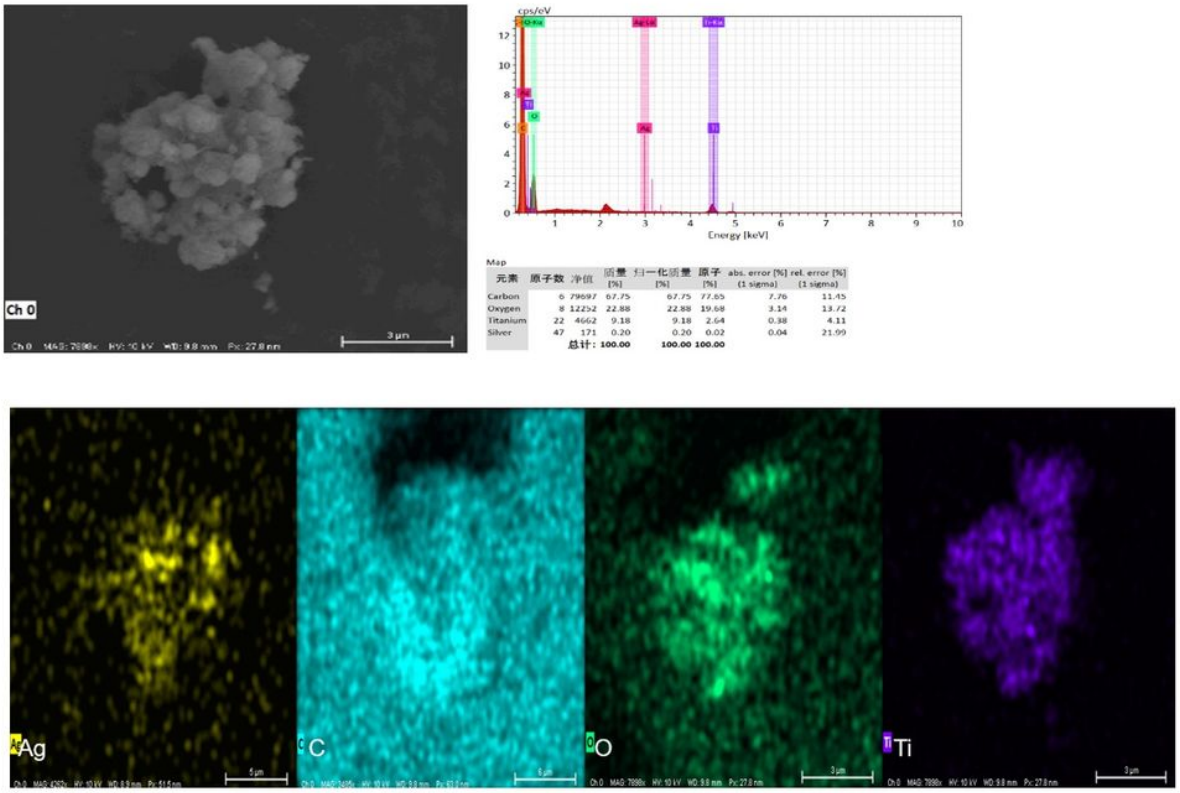

Figure 3

EDX diagram of CAT sample with 10% Ca mass fraction.

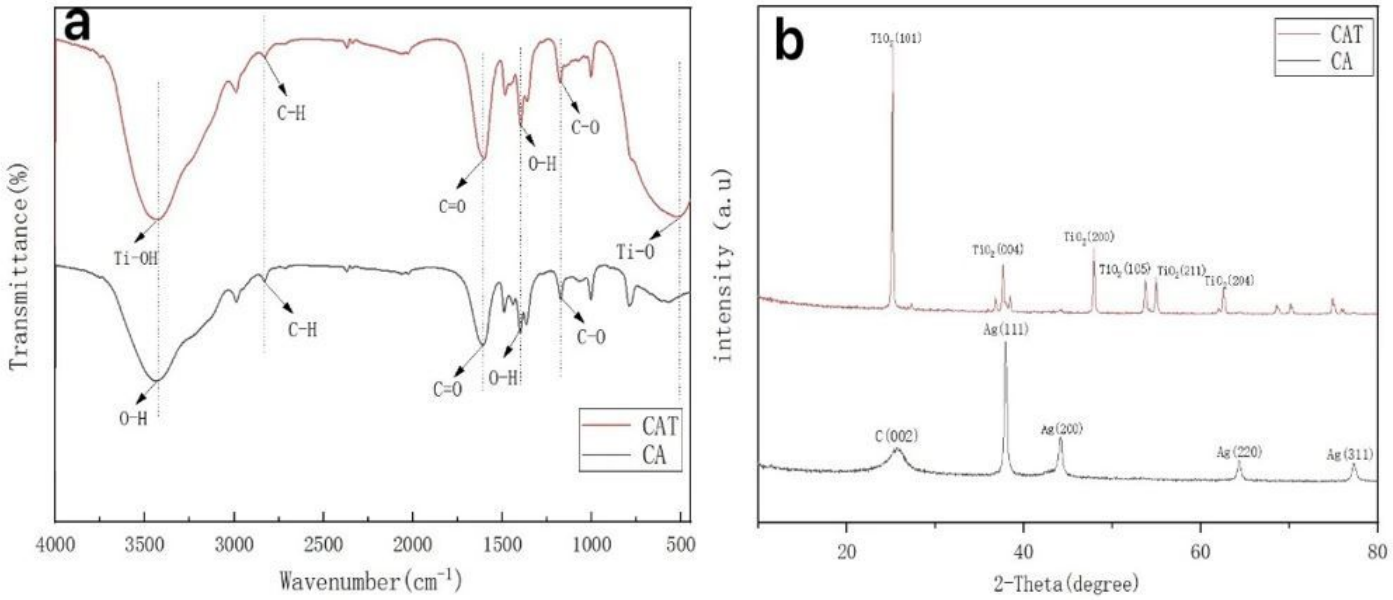

Figure 4

FTIR spectra (a) and XRD patterns (b) of CA and CAT.

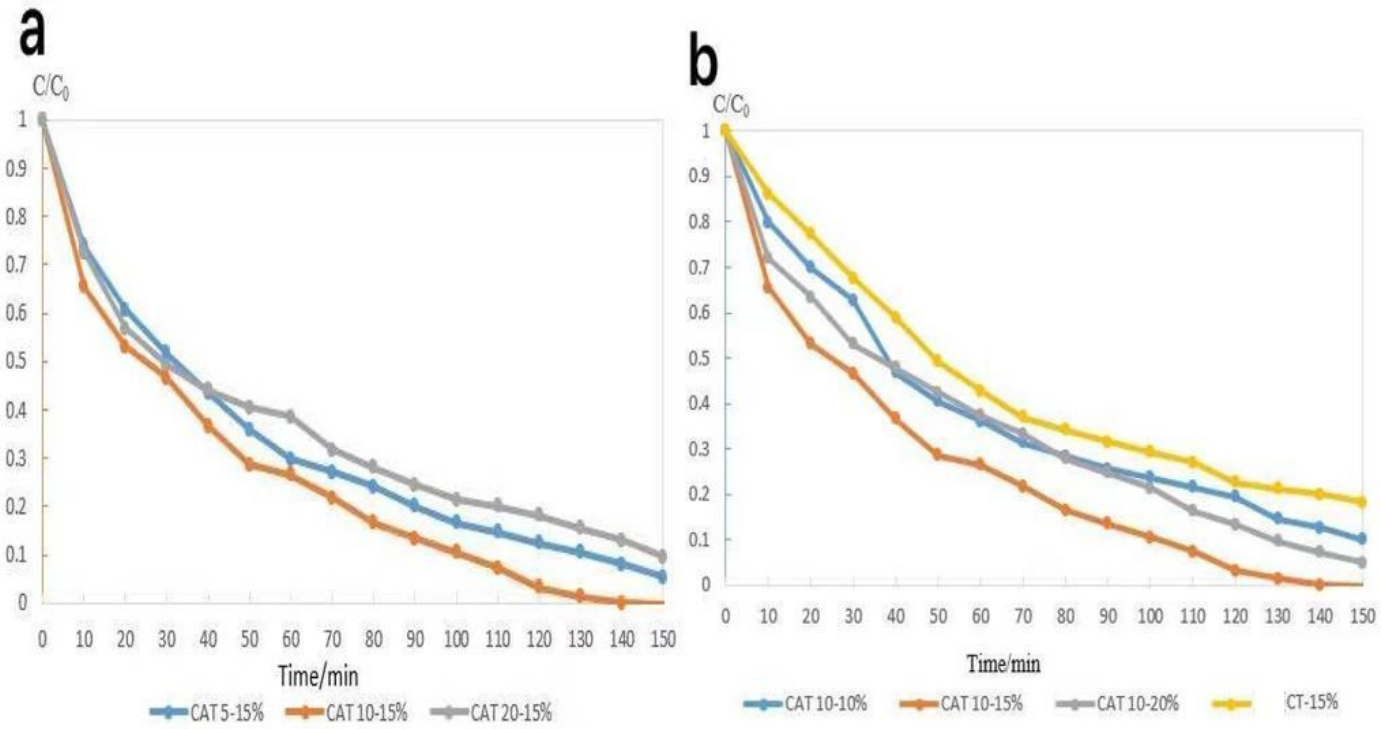

Figure 5

Degradation effect of CR by CAT （a）Degradation rate of CAT at different ratios of C:Ag（b）Degradation of CR wastewater by CAT with different CA treated amounts.

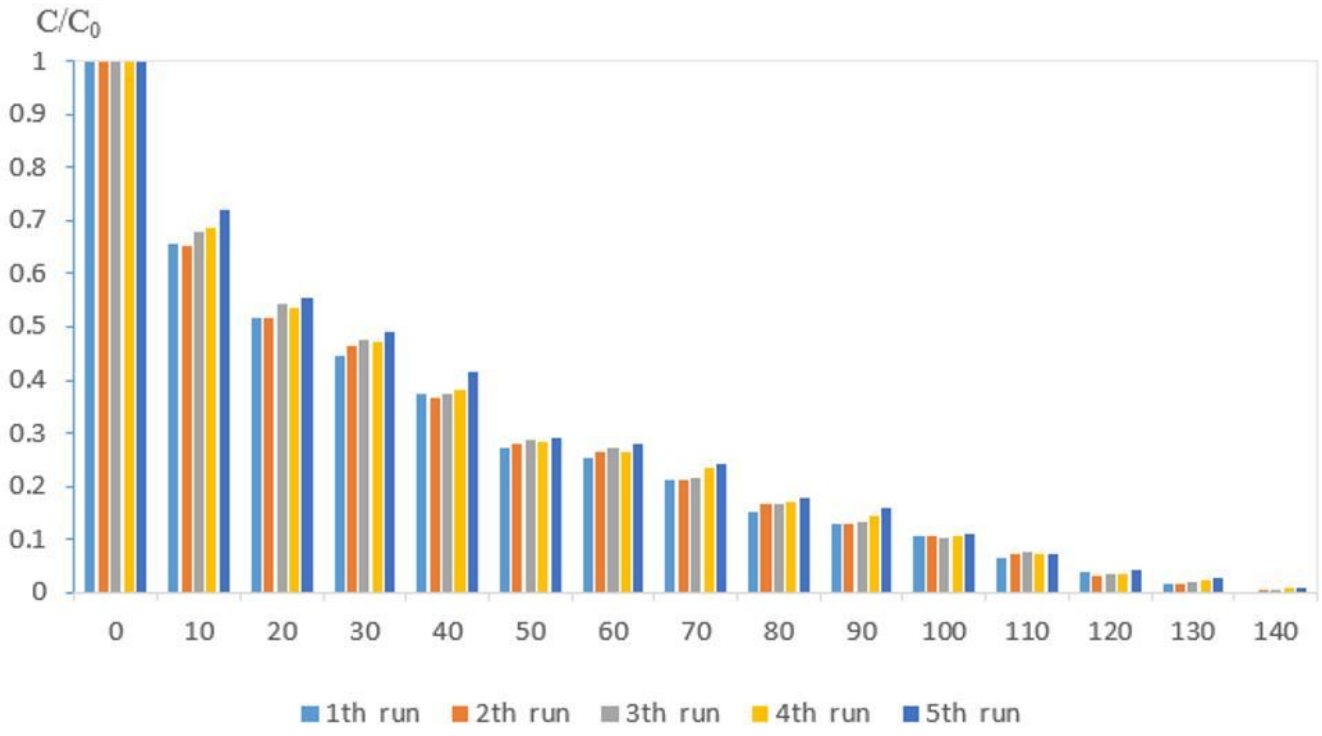

Figure 6

Cycling tests of 15% CAT

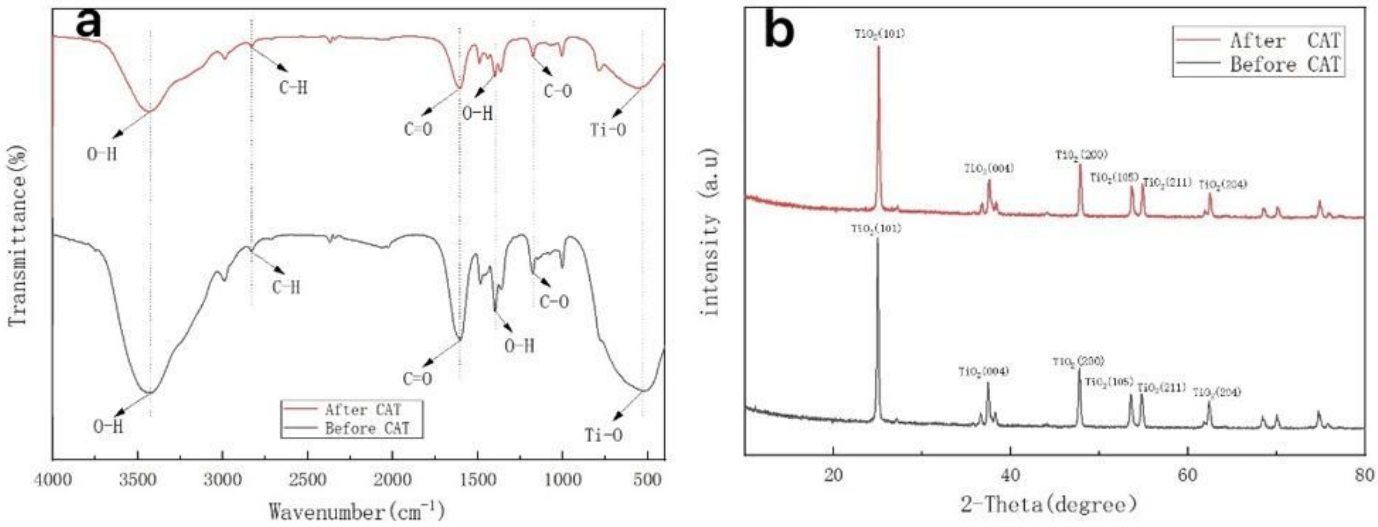

Figure 7

FTIR spectra (a) and XRD patterns (b) of CAT before and after reaction.